Dynamic and static response of multielectrode lasers

J. O'Gorman, A. F. J. Levi, R. N. Nottenburg, T. Tanbun-Ek,
and R. A. Logan
AT&T Bell Laboratories, Murray Hill, New Jersey 07974

(Received 19 April 1990; accepted for publication 20 June 1990)

We compare the measured and calculated light output of a semiconductor laser modulated by a saturable intracavity absorber. An accurate description of the dynamic and static behavior requires inclusion of both a carrier concentration dependent recombination rate and a voltage-dependent saturable absorption.

Recently we have explored the possibility of replacing some digital transistor circuits with optoelectronic components. One result of this effort has been demonstration of Gbit s^{-1} digital optoelectronic signal processing using multielectrode lasers.[1] These devices exhibit power gain[2] and as such may be considered as having transistor-like amplification characteristics. In contrast to a transistor however, the lasing light output is not decoupled from its driving source (the charge carrier density in the laser cavity) giving rise to undesirable relaxation oscillations in both the light intensity and the carrier density. In this letter we present a model of a multielectrode quantum well laser incorporating nonlinearities such as gain and absorber saturation and calculate their effect on the digital response of the device.

The single-mode rate equations for a laser structure of cavity length L_C, absorber section length L_S, stripe width W, and active region thickness d (see Fig. 1) may be written as

$$\frac{dn}{dt}=\frac{I_G}{ev}-R \tag{1}$$

and

$$\frac{dp}{dt}=\left(\Gamma G-\frac{1}{\tau_p'}\right)p+R_{\rm sp}, \tag{2}$$

where p is the photon density, n is the carrier density, R is the charge carrier recombination rate, G is the gain function, I_G is the gain current, $R_{\rm sp}$ is the spontaneous emission coupling into the lasing mode, $v=(L_C-L_S)Wd$ is the active region volume, Γ is the confinement factor and, $1/\tau_p'=(c/n_g)\alpha$, where n_g is the group velocity index of refraction, and α is the lumped loss of the laser. For a conventional semiconductor laser, constant carrier and photon lifetimes are generally assumed. With a multielectrode laser however, the cavity losses are determined by a voltage controlled loss modulator and consequently these assumptions cannot be made. We therefore write the recombination rate explicitly in terms of the carrier density

$$R=(A_{\rm nr}+Bn+Cn^2)n+Gp, \tag{3}$$

where $A_{\rm nr}$, B, and C describe nonradiative and radiative recombination processes in the semiconductor.[3] We note that the use of a carrier density dependent recombination time (in the absence of other factors such as gain saturation or spontaneous emission into the lasing mode) significantly dampens relaxation oscillations[4] and must be included in any realistic simulation of the dynamic behavior of semiconductor lasers. We assume that laser gain is a linear function of carrier density but is subject to gain saturation,[5] that is, $G=A(n-n_0)(1-\epsilon p)$, where n_0 is the carrier density required for transparency, A is the gain constant, and ϵ ($\ll 1.0$) is a gain saturation parameter. Spontaneous emission coupling into the lasing mode is given by $R_{\rm sp}=\beta\Gamma Bn^2$.

From the experimental pulsed light-current curve [Fig. 2(a)] it is apparent that the electroabsorption has both saturable and nonsaturable components. Specifically, in the above-threshold regime, an increase in the applied absorber voltage shifts the light-current curve to higher gain section currents. In addition, the laser displays an absorption saturation at threshold which is also a function of the applied voltage. We treat these saturable and nonsaturable elements as additive terms and write the total losses for the laser as

$$\alpha=\alpha_0+\alpha_m+\alpha_s(V)+\alpha_{\rm ns}(V) \tag{4}$$

where α_0 and α_m are, respectively, the familiar internal and mirror losses which determine laser threshold and differential quantum efficiency when the absorber section is forward biased, $\alpha_s(V)$ is the saturable loss and $\alpha_{\rm ns}(V)$ is the

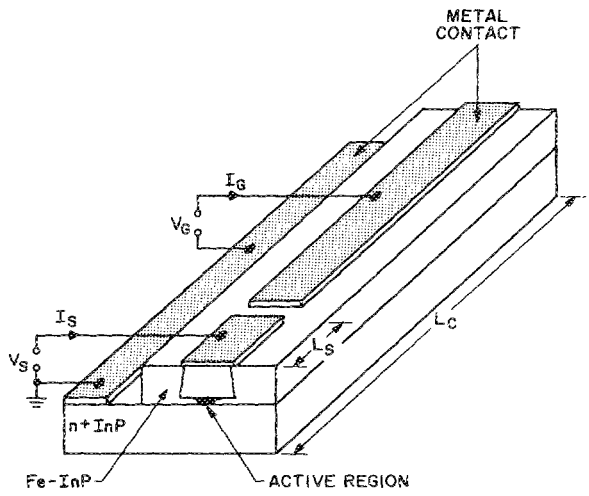

FIG. 1. Schematic sketch of a BH GRINSCH four quantum well laser diode with a cavity length L_C and an intracavity absorber of length L_S. The current into the long gain section is I_G, the absorber voltage and current are V_S and I_S, respectively.

 0003-6951/90/360968-03$02.00

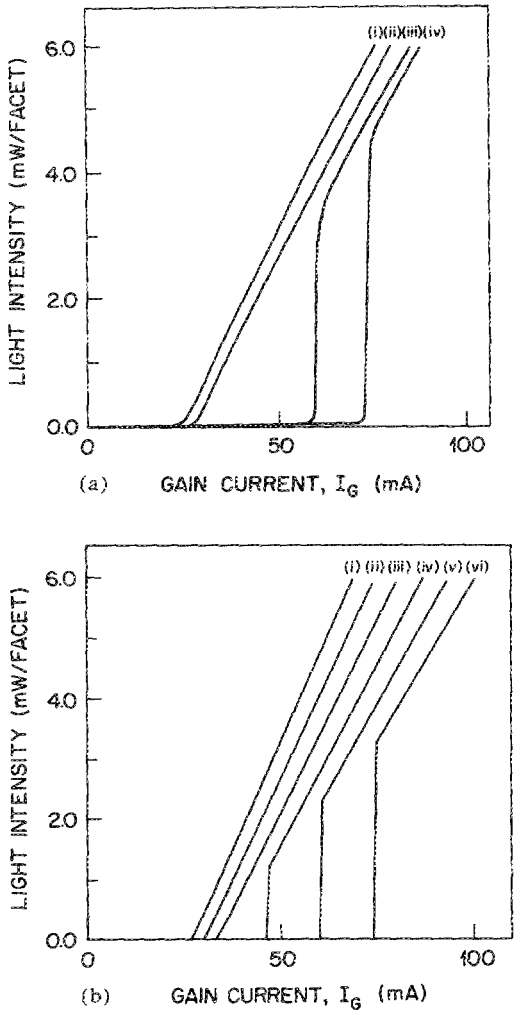

FIG. 2. (a) Measured light intensity per facet as a function of gain current, I_G, for various absorber voltages, V_S, (i) absorber section shorted to the gain section, (ii) $V_S = 0.8$ V, (iii) $V_S = 0.4$ V, and (iv) $V_S = 0.0$ V. (b) Calculated light intensity per facet as a function of gain current, I_G, for various absorber voltages, V_S. (i) $V_S = 1.0$ V, (ii) $V_S = 0.8$ V, (iii) $V_S = 0.6$ V, (iv) $V_S = 0.4$ V, (v) $V_S = 0.2$ V, and (vi) $V_S = 0.0$ V.

nonsaturable loss. Considering the absorbing section as a photon extractor, $\alpha_{ns}(V)$ is representative of the absorber extraction efficiency. Since the extrapolated threshold current changes in an approximately linear fashion with increasing absorber voltage we write $\alpha_{ns}(V) = \alpha_1 + \alpha_2 V$. Turning to the saturable loss, it is apparent in Fig. 2(a) (see also Ref. 2) that threshold current is an approximately linear function of applied absorber voltage. As the laser threshold is determined by saturation of the absorber we must conclude that saturable absorption is a function of applied voltage. It has recently been shown that nonlinear absorption in InGaAs/InAlAs quantum wells at a wavelength of $\lambda = 1.5$ μm is of the form $\alpha_s = \alpha_{s0}/(1 + I/I_s)$ where $I_S \sim 30$ kW cm^{-2}.[2,6,7] Furthermore, the experiments of Fox *et al.*[7] explicitly show that saturation intensity increases with increasing reverse bias voltage. This effect is attributed to a voltage dependence of carrier escape processes, such as recombination, thermionic emission, and quantum tunneling within the quantum well structure. Here we have assumed that, to a first approximation, I_S is

TABLE I. Parameters used to model a multielectrode BH GRINSCH four quantum well InGaAs/InP laser diode.

Parameter	Value
A	1.0×10^{-6} cm^3 s^{-1}
n_0	1.0×10^{18} cm^{-3}
A_{nr}	1.0×10^{8} s^{-1}
B	1.0×10^{-10} cm^3 s^{-1}
C	7.0×10^{-29} cm^6 s^{-1}
α_0	48.4 cm^{-1}
L_C	500.0 μm
W	2.0 μm
d	36.0 nm
n_g	4.0
β	1.0×10^{-5}
λ	1.5 μm
R_1	0.3
R_2	0.3
ϵ	2.0×10^{-17} cm^3
Γ	0.20
r_1	0.4
r_2	-0.26 V^{-1}
r_3	4.0
I_{S0}	30.0 kW cm^{-2}
κ	-1.20 V^{-1}

a linear function of applied voltage, i.e., $I_S = I_{S0}(1 + \kappa V)$. The total losses within the laser may now be conveniently written as

$$1/\tau_p' = (1/\tau_p)[1 + r_1 + r_2 V + r_3/(1 + I/I_s)], \qquad (5)$$

where $1/\tau_p + (c/n_g)(\alpha_0 + \alpha_m)$.

Equations (1)–(5) constitute our model. α_0 and α_m are obtained from the static light-current curve of the device with the absorber section forward biased, and r_1, r_2, and r_3 are treated as fitting parameters for devices of differing absorber and gain dimensions. In Fig. 2(b) we show a set of light-current curves calculated by integrating the rate equations, using the parameter values given in Table I and a set of applied absorber voltages in the range $0.0 \text{ V} \leqslant V_s \leqslant 1.0$ V for a buried-heterostructure graded index separate confinement heterostructure (BH GRINSCH) with four quantum wells and a cavity length, $L_C = 500$ μm.[1] The calculation accurately reproduces the observed Q-switched response of Fig. 2(a) and the variation in laser threshold with applied voltage. Obviously the voltage dependence of the saturation intensity plays a crucial role in determining the light-current characteristic of the device.

We have also simulated the dynamic behavior of the system. In Fig. 3(a) we show the experimentally observed response of a multielectrode laser when a 1 Gbit s^{-1} nonreturn to zero (NRZ) data stream is applied to the absorber section. The laser output is seen to follow the applied voltage with an approximately 100 ps turn-on delay, a purely digital response being impaired by a large relaxation oscillation which rides upon a square pedestal.

In Fig. 3(b) we show the calculated response of the laser to the same data stream as in Fig. 3(a) and using the same parameter values as used in Fig. 2(b).

Clearly, the agreement between calculation and experiment is excellent. It is to be noted furthermore that considerable damping of the relaxation oscillations is evident

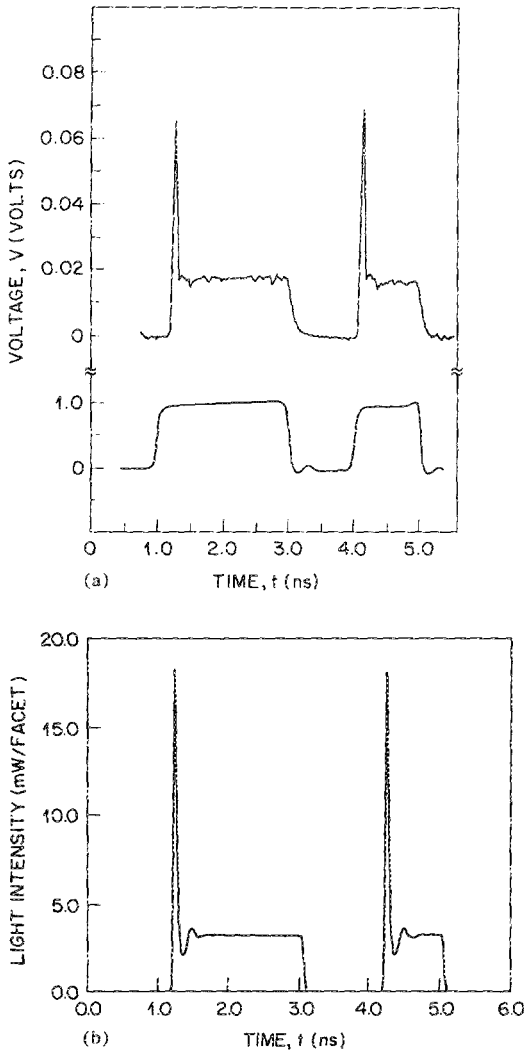

FIG. 3. (a) Oscilloscope trace of *p-i-n* receiver output (upper curve) to a ...011010... 1 Gbit s^{-1} NRZ data stream V_S (lower curve) applied to saturable absorber *S*. Data taken with $I_G = 70$ mA. (b) Calculated response of the multielectrode laser to a...011010.. 1 Gbit s^{-1} NRZ data stream applied to saturable absorber *S*.

even for very low levels of gain saturation. This is a direct consequence of the inclusion of the carrier recombination rate given by Eq. (3) above. The necessity of inclusion of a carrier density dependent recombination time is further

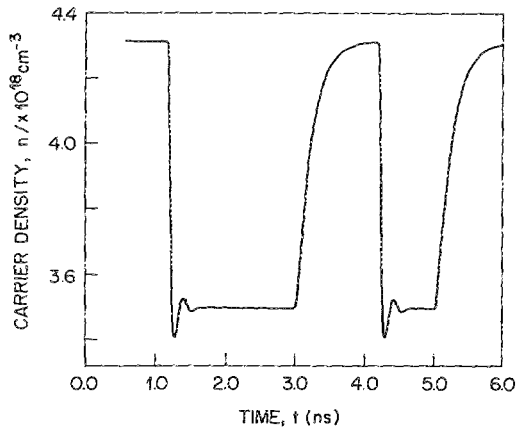

FIG. 4. Calculated variation in carrier density during application of a 1 Gbit s^{-1} NRZ data stream to saturable absorber *S*.

demonstrated in Fig. 4 where the calculated variation in carrier density during application of the data stream is reproduced.

In conclusion we have developed a model of a multielectrode quantum well laser incorporating gain nonlinearity and saturable absorption. We have utilized this model to investigate the static and dynamic behavior of the laser and have found good agreement between theory and experiment. Central to an accurate description of the device is the inclusion of a carrier concentration dependent recombination rate and a voltage-dependent saturable absorption.

[1] A. F. J. Levi, R. N. Nottenburg, R. A. Nordin, T. Tanbun-Ek, and R. A. Logan, Appl. Phys. Lett. **56**, 1095 (1990).
[2] K. Berthold, A. F. J. Levi, T. Tanbun-Ek, R. A. Logan, and S. N. G. Chu, Appl. Phys. Lett. **55**, 1940 (1989).
[3] G. P. Agrawal and N. K. Dutta, *Long Wavelength Semiconductor Lasers* (Van Nostrand-Reinhold, New York, 1986).
[4] B. J. Hawdon, J. O'Gorman, and D. M. Heffernan (unpublished).
[5] D. C. Channin, J. Appl. Phys. **50**, 3858 (1979).
[6] D. A. H. Mace, M. A. Fisher, M. G. Burt, E. G. Scott, and M. J. Adams, Opt. Lett. **15**, 189 (1990).
[7] A. M. Fox, D. A. B. Miller, G. Livescu, J. E. Cunningham, J. E. Henry, and W. Y. Jan (unpublished).